2-2017

Changes in temporal variability of precipitation over land due to anthropogenic forcings

Goutam Konapala
Clemson University

Ashok Mishra
Clemson University, ashokm@g.clemson.edu

L. Ruby Leung
Pacific Northwest National Laboratory

Changes in temporal variability of precipitation over land due to anthropogenic forcings

Environmental Research Letters

LETTER

Changes in temporal variability of precipitation over land due to anthropogenic forcings

Goutam Konapala[1], Ashok Mishra[1] and L Ruby Leung[2]

[1] Glenn Department of Civil Engineering, Clemson University, South Carolina, United States of America
[2] Pacific Northwest National Laboratory, Richland, Washington, United States of America

E-mail: ashokm@g.clemson.edu

Keywords: climate change, anthropogenic influence, precipitation variability

Supplementary material for this article is available online

OPEN ACCESS

RECEIVED
15 June 2016

REVISED
12 December 2016

ACCEPTED FOR PUBLICATION
4 January 2017

PUBLISHED
2 February 2017

Abstract

This study investigated the anthropogenic influence on the temporal variability of annual precipitation for the period 1950–2005 as simulated by the CMIP5 models. The temporal variability of both annual precipitation amount (PRCPTOT) and intensity (SDII) was first measured using a metric of statistical dispersion called the Gini coefficient. Comparing simulations driven by both anthropogenic and natural forcing (ALL) with simulations of natural forcing only (NAT), we quantified the anthropogenic contributions to the changes in temporal variability at global, continental and sub-continental scales as a relative difference of the respective Gini coefficients of ALL and NAT. Over the period of 1950–2005, our results indicate that anthropogenic forcing have resulted in decreased uniformity (i.e. increase in unevenness or disparity) in annual precipitation amount and intensity at global as well as continental scales. In addition, out of the 21 sub-continental regions considered, 14 (PRCPTOT) and 17 (SDII) regions showed significant anthropogenic influences. The human impacts are generally larger for SDII compared to PRCTOT, indicating that the temporal variability of precipitation intensity is generally more susceptible to anthropogenic influence than precipitation amount. The results highlight that anthropogenic activities have changed not only the trends but also the temporal variability of annual precipitation, which underscores the need to develop effective adaptation management practices to address the increased disparity.

1. Introduction

Understanding the anthropogenic contributions to climate change is an important aspect of climate science to advance our knowledge of the causes of the observed climatic trends and changes in extremes. Previous studies have established the anthropogenic influence on trends of climate variables, such as, precipitation (Zhang *et al* 2007), surface air temperature (Hegerl *et al* 1997, Zhang *et al* 2006), tropopause height (Santer *et al* 2003) and ocean heat content (Barnett *et al* 2005a, 2005b), among others. Some studies have highlighted the influence of human activities on individual extreme events, such as California's drought (Williams *et al* 2015), England's flood risk (Pall *et al* 2011) and European heat waves (Stott *et al* 2004, Otto *et al* 2012, Dole *et al* 2011) as well as the concurrence of multiple climate extremes (Min *et al* 2011, Angélil *et al* 2014, Fischer and Knutti 2015). Zhang *et al* (2013) and Zwiers *et al* (2011) identified the contribution of anthropogenic factors for intensification of precipitation extremes and prolonging return periods of daily temperature extremes.

Understanding the changes in annual precipitation is crucial for water resources planning to sustain agricultural, ecological and water infrastructure development in addition to protection of transport systems, homes and business infrastructure. Long term trends explain only one aspect of the changes occurring to annual precipitation. Combining the inter-annual and inter-decadal variability of precipitation and precipitation trends would give an overall picture of changes occurring in annual precipitation.

Previous studies established some linkages between annual and interannual-to-decadal variability of precipitation over land and natural modes of variability of the coupled climate system, such as El Nino–Southern Oscillation (ENSO), Arctic Oscillation (AO), and North Atlantic Oscillation (NAO), through teleconnection (Gu and Adler 2004, 2006, Medvigy *et al* 2008, Small and Islam 2008, Garreaud *et al* 2013). Global warming induced by anthropogenic forcing may alter the variability of precipitation. Simple thermodynamical argument in addition to circulation Changes (Schaller *et al* 2016) for 'wet gets wetter, dry gets drier' (Held and Soden 2006) and 'warm gets drier' (Xie *et al* 2010) suggests an increase in spatial heterogeneity of precipitation, as the increase in atmospheric precipitable water with warmer temperatures enhances moisture convergence or divergence in climatologically wet or dry regions. A similar heuristic argument would also suggest an increase in precipitation temporal variability would indicate an enhanced moisture convergence or divergence during wet or dry years.

A major source of uncertainty in the simple arguments used to scale changes in precipitation variability with warming is that they ignore potential changes in interannual or decadal modes of variability with warming and the teleconnection pathways that linked such changes to precipitation over land. Recent studies found a projected increase in the frequency of extreme ENSO event under GHG forcing (Cai *et al* 2014, 2015, Capotondi 2015), but the projected changes in spatial structure and amplitude of ENSO (e.g. Vecchi and Wittenberg 2010) and the precipitation response in the tropics and extra-tropics (Meehl and Teng 2007, Seager *et al* 2012) remain largely uncertain. By decomposing the model projected precipitation response to a canonical ENSO pattern of sea surface temperature variability into changes in the mean state of precipitation and the historical as well as a future enhancement in precipitation response to the canonical ENSO pattern, Bonfils *et al* (2015) identified regions that will likely experience precipitation anomalies that are without precedent in the current climate. These studies have provided a strong motivation to investigate the changes in precipitation temporal variability due to anthropogenic forcing in the past and future.

Estimating the changes in temporal variability of precipitation is complicated by uncertainty in the model simulations as well as the metrics used to define variability and detect its changes. This study attempts to estimate the changes in temporal variability of precipitation due to human contributions as well as quantifying its uncertainty. We introduce an index based on the Gini coefficient to quantify the anthropogenic influence on temporal variability of annual precipitation amount and intensity. The Gini coefficient is a measure of statistical dispersion that has been widely used in the field of economics as a measure of income inequality (Ceriani and Verme 2011). Recently, the Gini coefficient has also been applied in climate science (Masaki *et al* 2014, Rajah *et al* 2014). Unlike other measures, the Gini coefficient is not sensitive to the scale and probability distribution of the data, making it robust and easy to interpret (Rajah *et al* 2014, Ceriani and Verme 2011). We estimated the human contribution to potential changes in temporal precipitation variability at global and continental scales and to the Giorgi climate division (Giorgi 2000). The remainder of the paper is structured as follows: data description is in section 2, methods in section 3, and the results are presented in section 4, with discussions and conclusions provided in section 5.

2. Data

We utilized 42 realizations from 15 CMIP5 GCM models (see supplementary table T1 available at stacks.iop.org/ERL/12/024009/mmedia) to obtain 'annual total precipitation (PRCPTOT)' and 'simple precipitation intensity index (SDII)' from the CLIMDEX archive hosted by Canadian Centre for Climate Modeling and Analysis for the attribution analysis. PRCPTOT is defined as the total amount of precipitation on wet days (days with precipitation >1 mm). SDII is the annual precipitation intensity, obtained by dividing the total amount of precipitation in a year by the number of wet days in a year. PRCPTOT and SDII calculated from model simulations for historical (1950–2005) and historicalNat (1950–2005) were used to estimate the anthropogenic contribution to temporal variability. The historical simulations were driven by both time-dependent anthropogenic (greenhouse gas concentrations, aerosols and ozone and land use) and natural (solar and volcanic) forcing, while the historicalNat simulations were run only with the time-dependent natural forcing, hence providing estimates of the Earth's climate without anthropogenic influences. To compare the historical simulations, we utilized the observed dataset of the same variables obtained from HADEX2 dataset (Donat *et al* 2013) of CLIMDEX archive.

As the spatial resolution of the simulated precipitation variables from the GCMs varies, we have interpolated all the data to a common grid of resolution 2° latitude $\times$ 2° longitude using bilinear interpolation method. For temporal attribution, numerous studies (Zhang *et al* 2013, Westra *et al* 2013, Santer *et al* 2007) found that the signal-to-noise ratio of climate variables is enhanced by spatial averaging, resulting in a more statistically significant climate signal. Therefore, we used the spatial mean of the global land, continental land, and the Giorgi climate division (Giorgi and Francisco 2000) to obtain a single time series for each specific spatial unit.

3. Methodology

3.1. Gini coefficient

The Gini coefficient has been recently applied to quantify uniformity in time series of climate variables (Masaki *et al* 2014, Rajah *et al* 2014) and computed according to equation (1).

$$G = \frac{1}{n}\left(n + 1 - 2\left(\frac{\sum_{i=1}^{n}(n+1-i)y_i}{\sum_{i=1}^{n} y_i}\right)\right) \quad (1)$$

In our context, y_i indicates the PRCPTOT or SDII at a particular year i and n indicates the total number of years. The value of G theoretically varies between 0 and 1, with 0 corresponding to a complete uniformity (i.e. all the precipitation values are the same) and 1 corresponding to maximal non-uniformity or largest disparity (i.e. only a single annual precipitation amount is observed during the entire study period). So, smaller values of the Gini coefficient signify more uniformity in the temporal variation of precipitation. Figure 1 presents a pictorial derivation of the Gini coefficient. A brief discussion on comparison between Gini coefficient and traditional methods are provided in the supplementary information. Other methods like standard deviation and coefficient of variation are sensitive to scale and probability distribution of the data.

We also compared the Gini coefficient of the observed and simulated PRCPTOT and SDII to identify regions where there is an agreement (disagreement) in terms of their temporal variability (figure 2). The multi model ensemble mean of the Gini coefficient captures the variability of PRCPTOT in most regions. However, it underestimates the Gini coefficients in the Andes Mountain in South America and Himalayan mountains in Asia, while in the Middle East and India it is overestimated. Similarly, for SDII, better performance was observed in Europe, Western Asia, North America and South Africa. The models tend to overestimate the Gini coefficient in Middle Eastern Asia and western part of India. Due to limited precipitation data in many parts of Africa, Australia, the Amazon in South America and Greenland, we only showed the modeled variability in locations with observations for comparison. However, the supplementary figure S2 includes the coverage of all the land regions. To sum up, figures 2 and S2 show higher values of the Gini coefficient in most of the global arid regions. Overall, the good agreement between the Gini coefficients from observed and modeled annual precipitation variability in terms of both magnitude and intensity supports the use of the CMIP5 model outputs to quantify the anthropogenic contribution to changes in the temporal variability of PRCPTOT and SDII.

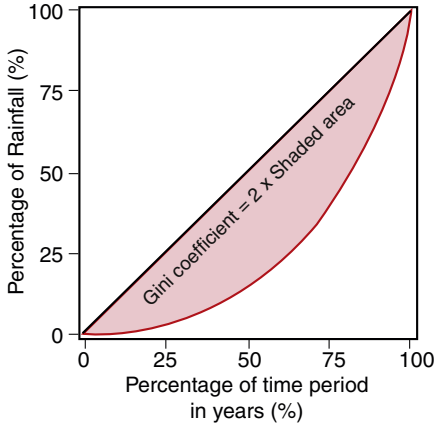

Figure 1. Pictorial explanation of the Gini coefficient for temporal variability: the annual precipitation amount is first ranked before being added cumulatively and converted to percentiles as shown by the red curve. The Gini value is then estimated as twice the area between the equality line (1 to 1 line) and the ranked distribution, depicted by the pink shaded area. Hence, the more pink an area is, the more the variability.

3.2. Relative anthropogenic index

A change between any two scenarios can be detected by evaluating their difference or the ratio of the corresponding model outputs. With this conceptual framework, several studies have evaluated the influence of greenhouse gases on tropical cyclone characteristics (Gualdi *et al* 2007) and tropospheric sulphate aerosol (Langner *et al* 1992). More recently, the fractional attributable risk (FAR) methodology (Stott *et al* 2004) based on the relative difference of probabilities was used to estimate the influence of anthropogenic forcing on heat waves (Pall *et al* 2011), climate extremes (Fischer and Knutti 2015, King *et al* 2015) and meteorological drought (Gudmundsson and Seneviratne 2016). This methodology quantifies the influence of anthropogenic forcing along with its statistical significance through bootstrapping. Likewise, we quantify the anthropogenic influence on temporal variability of precipitation via a change in the Gini coefficient. Here we define a Relative Anthropogenic Index (RAI) as the relative difference between the historical and HistoricalNat scenarios as follows:

$$\mathrm{RAI} = \frac{G_{\mathrm{ALL}} - G_{\mathrm{NAT}}}{G_{\mathrm{ALL}}} \quad (2)$$

Where, G_{ALL} and G_{NAT} represent the Gini coefficients of the anthropogenic plus natural forcing (ALL) and natural forcing only (NAT) simulations, respectively. A positive RAI indicates a decrease in annual precipitation variability, whereas a negative RAI indicates an increase in variability due to anthropogenic forcing. In the context of resource management, a positive RAI value implies increased challenges in managing water resources and ecosystems, whereas a negative value indicates reduced variability so water resources are more manageable. Also, as the RAI is a relative difference metric, a higher difference indicates more influence in positive as well negative RAI values.

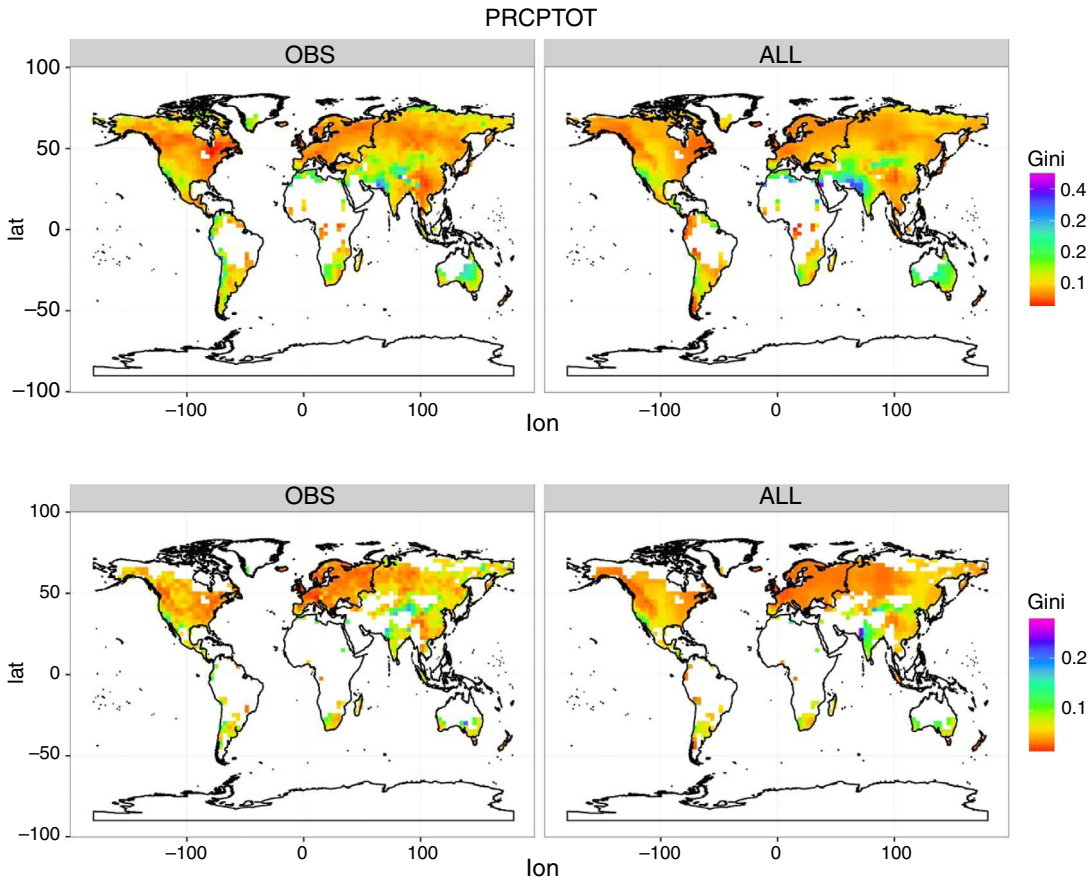

Figure 2. Comparison between observed (OBS) and multi model ensemble mean (ALL) Gini coefficients for PRCPTOT (mm/year) and SDII (mm/day) indices. The GCM data is masked to show only those regions where observed data is available for better representation.

We calculated the RAI for a specified spatial unit by first spatially averaging the gridded Gini coefficients over the specified region for a particular scenario and realization. Therefore, each spatial unit has a single Gini value for each CMIP5 realization separately for the ALL and NAT scenarios. Then we estimated the RAI as explained by equation (2) by using the multi model ensemble means of 42 CMIP5 realizations. In order to estimate uncertainty in the RAI values, we used the Bootstrapping resampling procedure (Efron and Tibshirani 1994) to generate 10 000 sub-samples from the 42 CMIP5 realizations and ranked them to extract the 5th percentile and 95th percentile RAI values. A positive RAI median is statistically significant if its 5th percentile value is also positive. Similarly, for negative RAI median to be statistically significant, the 95th percentile value should also be negative (Fischer and Knutti 2015, King *et al* 2015). Hence, the RAI estimates the influence of anthropogenic forcings on the temporal variation along with its significance. To further aid the significance of RAI, a two sample t-test on the G_{ALL} and G_{NAT} resamples was performed and reported in the supplementary information.

4. Results

For global land analysis, the Gini coefficients are calculated separately for the ALL and NAT scenarios over all the land regions as mentioned in section 3.1 for all the 42 GCM realizations and averaged spatially. Then through the process of bootstrapping, we randomly selected GCM models with repetition from the pool of 42 GCM models considered and computed their ensemble means. This process was repeated 10 000 times to obtain 10 000 spatially averaged Gini coefficients that represent the inter-model variability. The probability distributions of the globally averaged bootstrap resampled Gini coefficients derived from the multi-model ensemble global land means were plotted in figure 3 (top panel). This represents the inter-model GCM spread of the estimated global land averaged Gini coefficients. The RAI was then computed for all the resampled (shown in the top panel) Gini coefficients and from its distribution the median and 95th percentile values were determined as shown in figure 3 (bottom panel). We used the median RAI value obtained from this bootstrapped distribution as our best estimate in all our discussions. There is an increase in RAI for PRCPTOT (0.11) and SDII (0.14), which indicates higher temporal variability due to anthropogenic contributions at global scale. This result indicates a statistically significant (95% confidence) increase in non-uniformity of PRCPTOT and SDII by 11% and 14%, respectively due to anthropogenic forcings.

Figure 4 shows the best RAI (i.e. median value) estimates at continental scale along with their 95% and

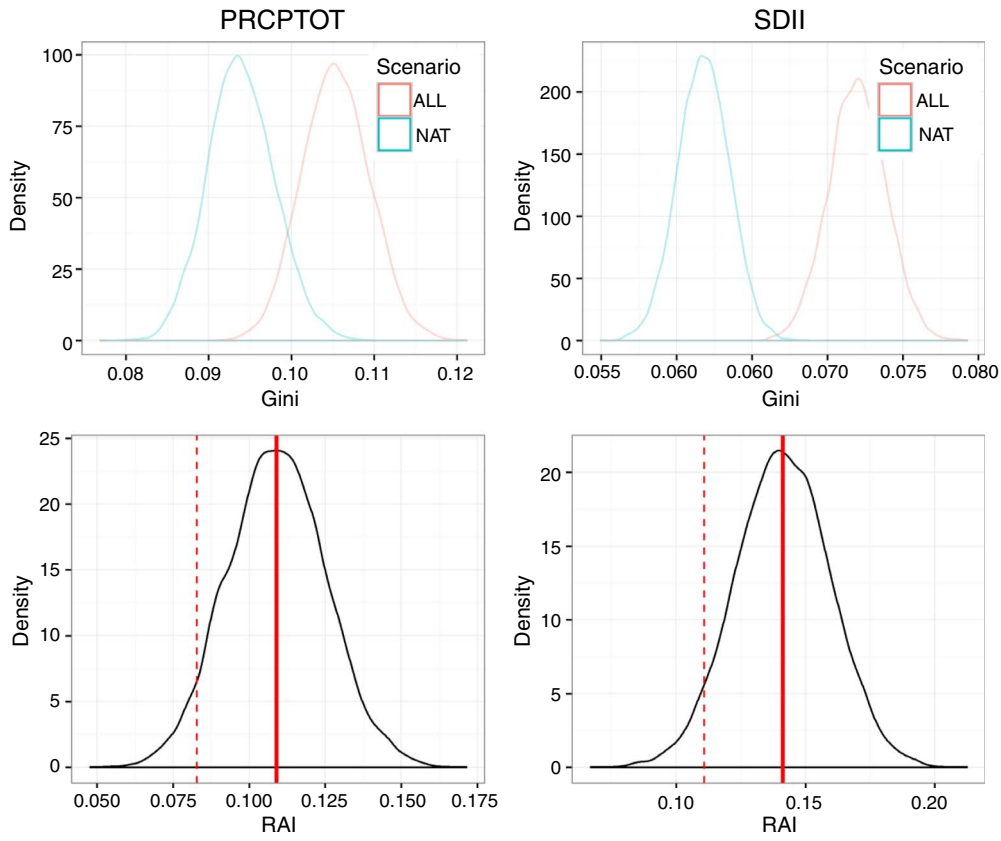

Figure 3. The figure on the top panel shows the probability distribution of the resampled global land averaged Gini coefficients for ALL and NAT scenarios obtained by the bootstrapping procedure explained in section 3.1. The bottom panel represents the distribution of RAI values for PRCPTOT (mm/year) and SDII (mm/day) as obtained from utilizing the ALL and NAT scenarios from the top panels. The solid red line indicates the median (best estimate) value of RAI and the dashed line indicates the 95th percentile value.

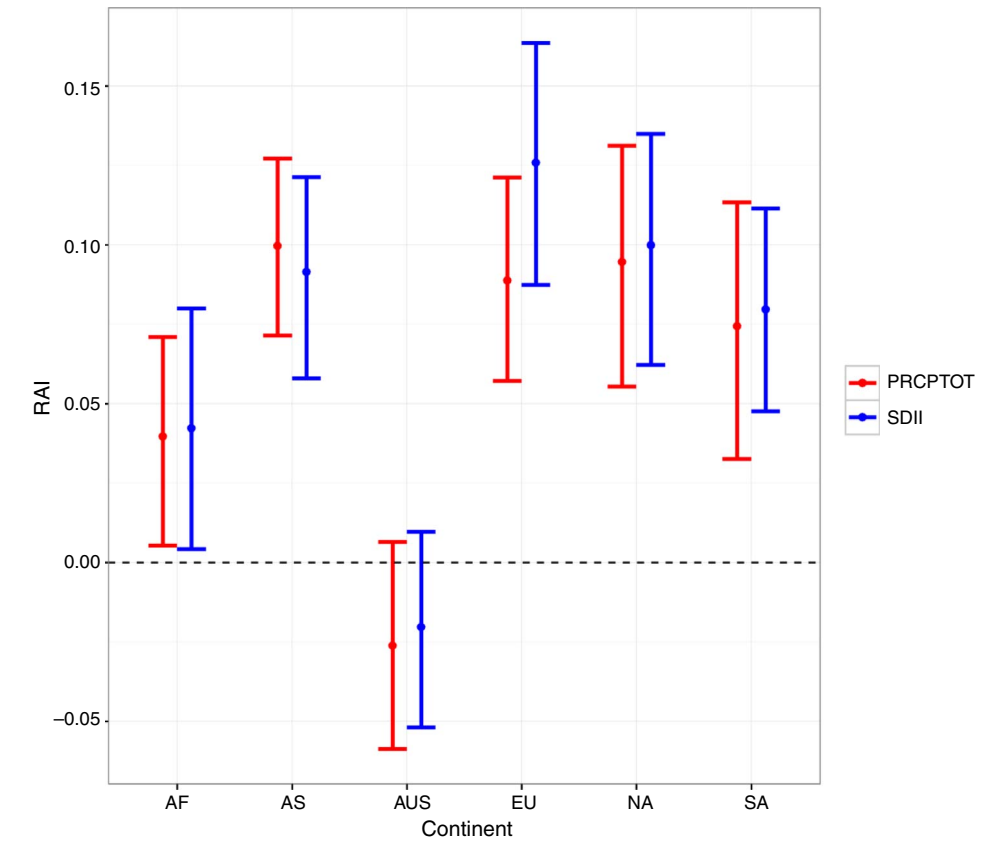

Figure 4. The temporal RAI estimates of PRCPTOT (red) and SDII (blue) calculated from spatially averaged over continents. In the figure, the median (solid dot) represents best estimates derived based on bootstrapping procedure.

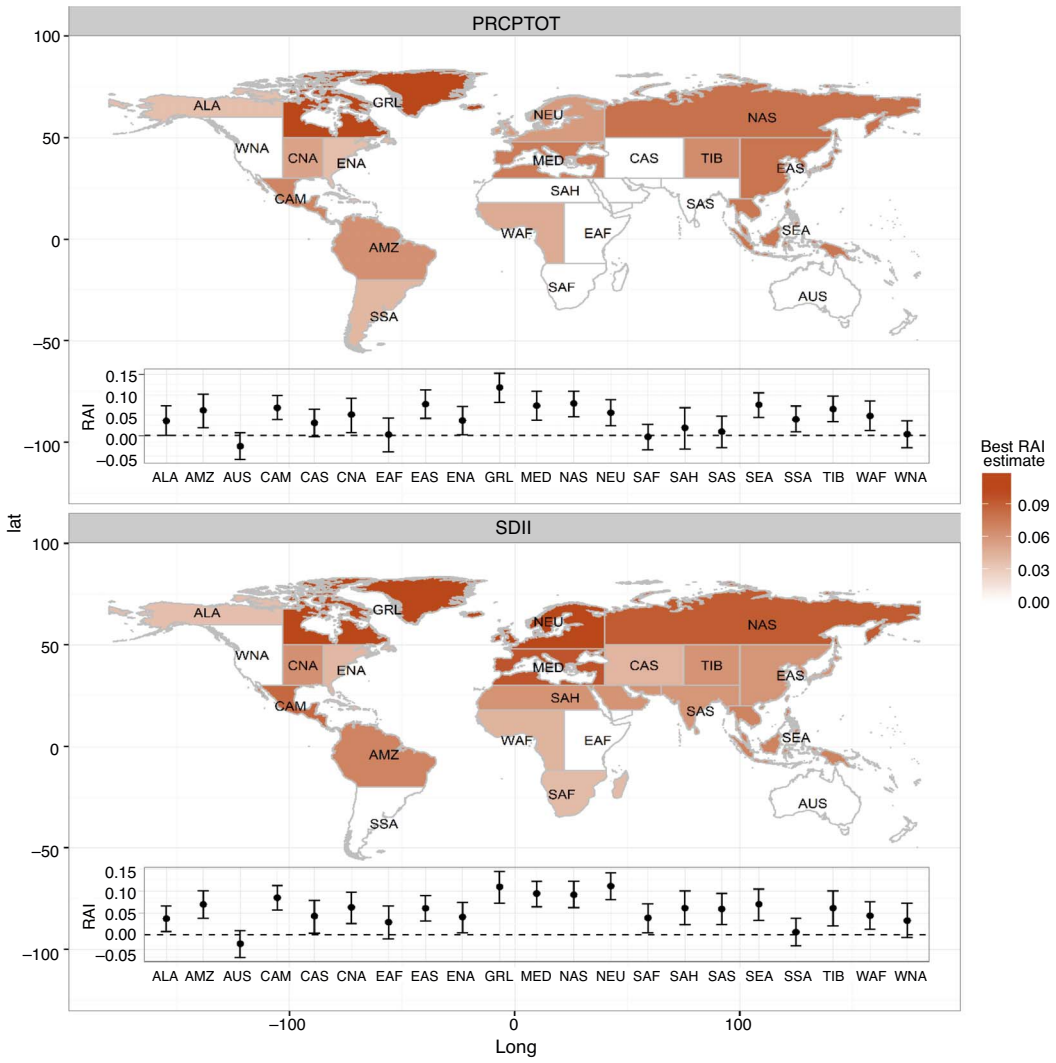

Figure 5. The best temporal RAI estimates calculated based on the bootstrapping procedure for PRCPTOT (mm/year) and SDII (mm/day) over sub-continental Giorgi regions. The inserted figure represents the uncertainty range (5th to 95th percentile) of RAI and the solid dot represents best estimate (i.e. median value). Only the RAI estimates of the significant regions are shown.

5% limits. The RAI values for all continents except Australia (AUS) are significantly greater than zero for both PRCPTOT and SDII. Europe (EU), Asia (AS) and North America (NA) register higher temporal variability of SDII and PRCPTOT respectively due to anthropogenic forcing in comparison to all other continents. Furthermore, all continents exhibit small differences in anthropogenic influence on temporal variability between PRCPTOT and SDII with the exception of Europe (EU). Australia (AUS) does not exhibit a statistically significant change in temporal variability of both PRCPTOT and SDII. The best estimate RAI value for the African (AF), Asian (AS) and North American (NA) and South American (SA) continents indicates that asymmetry has increased in SDII and PRCPTOT due to anthropogenic forcing by a factor of 0.04, 0.1, 0.1 and 0.08 (4%, 10%, 10%, 8% increase) respectively.

Figure 5 shows the best RAI estimates in the Giorgi regions along with their uncertainty range at 95% and 5% limits. Among all the Giorgi climate divisions, the GRL region located in North America exhibits higher anthropogenic influence on the variability of both PRCPTOT and SDII. The NEU region located in the European continent exhibits the largest difference of anthropogenic influence on the variability between PRCPTOT and SDII. However, EAF, SAF, SAH, SAS and WNA exhibit statistically insignificant anthropogenic influence on PRCPTOT. Similarly, for SDII, the regions of ENA, WNA and SSA exhibit insignificant anthropogenic influence. Overall, larger RAI values for SDII compared to PRCPTOT indicate that the temporal variability of precipitation intensity is more susceptible to anthropogenic disturbances than precipitation amounts. The African continent has more number of regions with insignificant anthropogenic induced non-uniformity. Both regions located in Europe show an average RAI value of 0.11 and 0.7 for SDII and PRCPTOT, respectively, indicating that Europe may have higher anthropogenic induced

non-uniformity among all the continents. Asia and North America have also exhibited more number of regions with significant anthropogenic induced changes in temporal variability.

From a physical perspective, warming in the historical period could lead to an increase in total precipitation due to an increased water holding capacity in the atmosphere. For example, climate models projected an increase of global mean precipitation by about 2% per degree warming in the future (Held and Soden 2006). Regionally, precipitation changes are more variable. The difference in the Gini coefficient between the ALL forcing and NAT forcing simulations could potentially reflect the trends in response to warming in the ALL forcing simulations. To investigate if a larger magnitude of trend increases the Gini value, we calculated the linear trends of the multi-model ensemble mean for PRCPTOT and SDII in all 42 historical realizations for the period 1951 to 2005. The linear trend magnitude calculated using the absolute value of Sen's slope (Sen 1968) and its correlation with the Gini coefficient are shown in supplementary figure S3. The coefficient of determination (R^2) between the linear trend magnitudes and the Gini coefficients is 0.0058 and 0.0067 for PRCTOT and SDII, respectively. These results indicate that statistically there is no linear relation between the magnitude of long-term linear trends and the Gini coefficients, suggesting that the differences in the Gini coefficients between the ALL forcing and NAT forcing simulations are not solely reflecting annual precipitation trends, but also changes in the interannual and/or interdecadal variability in annual precipitation and precipitation intensity.

5. Discussion and conclusions

Recognizing that anthropogenic forcing could have a significant influence on the temporal variability of precipitation amounts (PRCPTOT) and intensity (SDII), this study used the Gini coefficient to detect changes in the temporal variability of annual precipitation. By comparing CMIP5 simulations with ALL and NAT forcing, we found a clear signal indicating a significant anthropogenic influence on the temporal variability of PRCPTOT and SDII at global scale. The same is true at continental scale except for the Australian continent, where natural variability induced by various teleconnections (Risbey *et al* 2009, King *et al* 2014) is more dominant. Despite the lack of a signal in temporal variability, the decrease in Australian precipitation has been attributed to anthropogenic forcing (Timbal *et al* 2006 and Delworth and Zeng 2014), consistent with the understanding that processes influence the trend and variability of PRCPTOT and SDII could be very different.

Out of the 21 Giorgi regions, we found 14 (PRCPTOT) and 17 (SDII) regions showing significant anthropogenic influences. The human impacts are generally larger for SDII compared to PRCTOT. This indicates that at regional scale, the temporal variability of precipitation intensity is generally more susceptible to anthropogenic influence than precipitation amount. Areas with higher precipitation magnitude (such as: SEA, AMZ and WAF) and low precipitation magnitude (such as: SAH, CAS) have both witnessed an increase in non-uniformity in temporal variability of annual precipitation due to anthropogenic forcing. Regions with statistically insignificant anthropogenic influence on PRCPTOT are mostly monsoon-dominated regions that exhibit higher natural variability related to ENSO and other modes of variability (Wang and Ding 2008, Lee and Wang 2014). This may be reflecting uncertainties in model simulations of interannual and decadal modes of variability as well as how they respond to anthropogenic forcing, opposing influence of circulation and moisture changes on precipitation variability, or the precipitation variability changes due to anthropogenic influences have not emerged due to small signal-to-noise ratios in the historical period. This highlights the need for further investigation on changes in precipitation temporal variability as anthropogenic forcing continues to increase in the future.

Overall our results indicate that anthropogenic emissions have not only influenced the trends of annual precipitation (Zhang *et al* 2007), but their influence can be detected on the temporal variability of annual precipitation amount as well as intensity. Both PRCPTOT and SDII have significant implications for the net primary production of terrestrial ecosystems (Estiarte *et al* 2016) and agricultural yields (Thornton *et al* 2014). Hence an increased temporal variability in PRCPTOT and SDII would increase the complexity in formulating policy for water resources planning and management.

Acknowledgments

AM and GK are supported by the National Science Foundation (NSF) grant #1602451. LRL was supported by the U.S. Department of Energy (DOE) Office of Science Biological and Environmental Research as part of the Regional and Global Climate Modeling program. PNNL is operated for DOE by Battelle Memorial Institute under contract DE-AC05-76RL01830. We acknowledge the World Climate Research Programme's Working Group on Coupled Modelling for CMIP5 data used in the study. We acknowledge the CLIMDEX project maintained by the researchers at the Climate Change Research Centre, The University of New South Wales, for providing the CMIP5 model indices and runs, and the HadEX2 data set.

References

Allen M and Ingram W 2002 Constraints on future changes in climate and the hydrologic cycle *Nature* **419** 224–32

Angélil O, Stone D A, Tadross M, Tummon F, Wehner M and Knutti R 2014 Attribution of extreme weather to anthropogenic greenhouse gas emissions: sensitivity to spatial and temporal scales *Geophys. Res. Lett.* **41** 2150–5

Barnett T, Zwiers F, Hegerl G, Allen M, Crowley T, Gillett N, Hasselmann K, Jones P, Santer B and Schnur R 2005a Detecting and attributing external influences on the climate system: a review of recent advances *J. Clim.* **18** 1291–314

Barnett T P, Pierce D W, Achutarao K M, Gleckler P J, Santer B D, Gregory J M and Washington W M 2005b Penetration of human-induced warming into the world's oceans *Science* **309** 284–7

Bonfils C J W, Santer B D, Phillips T J, Marvel K, Leung L R, Doutriaux C and Capotondi A 2015 Relative contributions of mean-state shifts and ENSO-driven variability to precipitation changes in a warming climate *J. Clim.* **28** 9997–10013

Cai W *et al* 2014 Increasing frequency of extreme El Niño events due to greenhouse warming *Nat. Climate Change* **4** 111–6

Cai W *et al* 2015 Increased frequency of extreme La Niña events under greenhouse warming *Nat. Climate Change* **5** 132–7

Capotondi A 2015 Atmospheric science: extreme La Niña events to increase *Nat. Climate Change* **5** 100–1

Ceriani L and Verme P 2011 The origins of the Gini index: extracts from Variabilità e Mutabilità 1912 by Corrado Gini *J. Econ. Inequal.* **10** 421–43

Delworth T L and Zeng F 2014 Regional rainfall decline in Australia attributed to anthropogenic greenhouse gases and ozone levels *Nat. Geosci.* **7** 583–7

Donat M G *et al* 2013 Updated analyses of temperature and precipitation extreme indices since the beginning of the twentieth century: the HadEX2 dataset *J. Geophys. Res.: Atmos.* **118** 2098–18

Dole R *et al* 2011 Was there a basis for anticipating the 2010 Russian heat wave?. *Geophys. Res. Lett.* **38** L06702

Efron B and Tibshirani R J 1994 *An Introduction to the Bootstrap* (Boca Raton, FL: CRC Press)

Estiarte M *et al* 2016 Few multi-year precipitation-reduction experiments find a shift in the productivity-precipitation relationship *Glob. Change Biol.* **22** 2570–81

Fischer E M and Knutti R 2015 Anthropogenic contribution to global occurrence of heavy-precipitation and high-temperature extremes *Nat. Clim. Change* **5** 560–4

Garreaud R, Lopez P, Minvielle M and Rojas M 2013 Large-scale control on the Patagonian climate *J. Clim.* **26** 215–30

Giorgi F and Francisco R 2000 Uncertainties in regional climate change prediction: a regional analysis of ensemble simulations with the HADCM2 coupled AOGCM *Clim. Dynam.* **16** 169–82

Gualdi S, Scoccimarro E and Navarra A 2007 Changes in tropical cyclone activity due to global warming: results from a high-resolution coupled general circulation model *CMCC Research Paper* (https://doi.org/10.1175/2008JCLI1921.1)

Gudmundsson L and Seneviratne S I 2016 Anthropogenic climate change affects meteorological drought risk in Europe *Environ. Res. Lett.* **11** 044005

Gu G and Adler R F 2004 Seasonal evolution and variability associated with the West African monsoon system *J. Clim.* **17** 3364–77

Gu G and Adler R F 2006 Interannual rainfall variability in the tropical Atlantic region *J. Geophys. Res.: Atmos.* **111** D02106

Hegerl G C, Hasselmann K, Cubasch U, Mitchell J, Roeckner E, Voss R and Waszkewitz J 1997 Multi-fingerprint detection and attribution analysis of greenhouse gas, greenhouse gas-plus-aerosol and solar forced climate change *Clim. Dyn.* **13** 613–34

Held I M and Soden B J 2006 Robust responses of the hydrological cycle to global warming *J. Clim.* **19** 5686–99

King A D, Klingaman N P, Alexander L V, Donat M G, Jourdain N C and Maher P 2014 Extreme rainfall variability in Australia: patterns, drivers, and predictability *J. Clim.* **27** 6035–50

King A D, van Oldenborgh G J, Karoly D J, Lewis S C and Cullen H M 2015 Attribution of the record high Central England temperature of 2014 to anthropogenic influences *Environ. Res. Lett.* **10** 054002

Langner J, Rodhe H, Crutzen P J and Zimmermann P 1992 Anthropogenic influence on the distribution of tropospheric sulphate aerosol *Nature* **359** 712–6

Lee J and Wang B 2014 Future change of global monsoon in the CMIP5 *Clim. Dyn.* **42** 101–19

Masaki Y, Hanasaki N, Takahashi K and Hijioka Y 2014 Global-scale analysis on future changes in flow regimes using Gini and Lorenz asymmetry coefficients *Water Resour. Res.* **50** 4054–78

Medvigy D, Walko R and Avissar R 2008 Modeling interannual variability of the Amazon hydroclimate *Geophys. Res. Lett.* **35** L15817

Meehl G and Teng H 2007 Multi-model changes in El Niño teleconnections over North America in a future warmer climate *Clim. Dyn.* **29** 779–90

Min S K, Zhang X, Zwiers F W and Hegerl G C 2011 Human contribution to more-intense precipitation extremes *Nature* **470** 378–81

Otto F E, Massey N, Oldenborgh G J, Jones R G and Allen M R 2012 Reconciling two approaches to attribution of the 2010 Russian heat wave *Geophys. Res. Lett.* **39** L04702

Pall P, Aina T, Stone D A, Stott P A, Nozawa T, Hilberts A G, Lohmann D and Allen M R 2011 Anthropogenic greenhouse gas contribution to flood risk in England and Wales in autumn 2000 *Nature* **470** 382–5

Rajah K, O'Leary T, Turner A, Petrakis G, Leonard M and Westra S 2014 Changes to the temporal distribution of daily precipitation *Geophys. Res. Lett.* **41** 8887–94

Risbey J S, Pook M J, McIntosh P C, Wheeler M C and Hendon H H 2009 On the remote drivers of rainfall variability in Australia *Mon. Weather Rev.* **137** 3233–53

Santer B D *et al* 2007 Identification of human-induced changes in atmospheric moisture content *Proc. Natl Acad. Sci. USA* **104** 15248–53

Santer B D *et al* 2003 Contributions of anthropogenic and natural forcing to recent tropopause height changes *Science* **301** 479–83

Schaller N *et al* 2016 Human influence on climate in the 2014 Southern England winter floods and their impacts *Nat. Clim. Change* **6** 627–34

Seager R, Naik N and Vogel L 2012 Does global warming cause intensified interannual hydroclimate variability? *J. Clim.* **25** 3355–72

Sen P K 1968 Estimates of the regression coefficient based on Kendall's Tau *J. Am. Stat. Assoc.* **63** 1379–89

Small D and Islam S 2008 Low frequency variability in fall precipitation across the United States *Water Resour. Res.* **44** W04426

Stott P A, Stone D A and Allen M R 2004 Human contribution to the European heatwave of 2003 *Nature* **432** 610–4

Thornton P K, Ericksen P J, Herrero M and Challinor A J 2014 Climate variability and vulnerability to climate change: a review *Glob. Change Biol.* **20** 3313–28

Timbal B, Arblaster J M and Power S 2006 Attribution of the late-twentieth-century rainfall decline in southwest Australia *J. Clim.* **19** 2046–62

Vecchi G and Wittenberg A 2010 El Niño and our future climate: where do we stand? *Wiley Interdiscip. Rev.: Clim. Change* **1** 260–70

Wang B and Ding Q 2008 Global monsoon: dominant mode of annual variation in the tropics *Dyn. Atmos. Oceans* **44** 165–83

Westra S, Alexander L V and Zwiers F W 2013 Global increasing trends in annual maximum daily precipitation *J. Clim.* **26** 3904–18

Williams A P, Seager R, Abatzoglou J T, Cook B I, Smerdon J E and Cook E R 2015 Contribution of anthropogenic warming to California drought during 2012–2014 *Geophys. Res. Lett.* **42** 6819–28

Xie S P, Deser C, Vecchi G A, Ma J, Teng H and Wittenberg A T 2010 Global warming pattern formation: Sea surface temperature and rainfall *J. Clim.* **23** 966–86

Zhang X, Wan H, Zwiers F W, Hegerl G C and Min S 2013 Attributing intensification of precipitation extremes to human influence *Geophys. Res. Lett.* **40** 5252–7

Zhang X, Zwiers F W, Hegerl G C, Lambert F H, Gillett N P, Solomon S, Stott P A and Nozawa T 2007 Detection of human influence on twentieth-century precipitation trends *Nature* **448** 461–5

Zhang X, Zwiers F W, Hegerl G C, Lambert F H, Gillett N P, Solomon S, Stott P A and Nozawa T 2007 Detection of human influence on twentieth-century precipitation trends *Nature* **448** 461–5

Zhang X, Zwiers F W and Stott P A 2006 Multimodel multisignal climate change detection at regional scale *J. Clim.* **19** 4294–307

Zwiers F W, Zhang X and Feng Y 2011 Anthropogenic influence on long return period daily temperature extremes at regional scales *J. Clim.* **24** 881–92